Research Article

Efficient numerical methods on modified graded mesh for singularly perturbed parabolic problem with time delay

A. Kumar and S. Gowrisankar*,

Abstract

In this article, we develop an efficient numerical method for one-dimensional time-delayed singularly perturbed parabolic problems. The proposed numerical approach comprises an upwind difference scheme with modified graded mesh in the spatial direction and a backward Euler scheme on uniform mesh in the temporal direction. In order to capture the local behavior of the solutions, stability and error estimations are obtained with respect to the maximum norm. The proposed numerical method converges uniformly with first-order up to logarithm in the spatial variable and also first-order in the temporal variable. Finally, the outcomes of the numerical experiments are included for two test problems to validate the theoretical findings.

*Corresponding author

Received 11 May 2023; revised 18 August 2023; accepted 19 August 2023

Ankesh Kumar

Department of Mathematics, National Institute of Technology Patna, Patna - 800005, India. e-mail: ankeshk.phd19.ma@nitp.ac.in

S. Gowrisankar

Department of Mathematics, National Institute of Technology Patna, Patna - 800005, India. e-mail: s.gowri@nitp.ac.in

1 Introduction

Singularly perturbed problems are widely applicable in different fields of science and engineering. In particular, singularly perturbed convection-diffusion parabolic equations, which contain a small parameter and a delay term, are effective in the simulation of reservoirs subsurface oil extraction, convective heat transfer problems with high péclet numbers, fluid flows, mathematical biology, and so on. Problems with delay have also appeared in the study of tumor growth, neural networks, and also in problems related to the respiratory system. The dynamics of the delay differential equations may become complicated due to time delay as it alters the stability equilibrium of the system. In epidemiology, to denote the incubation time or the host infection time, delay can be used. From the statistical study of ecological data, it is revealed that delay effects are seen in many species' population dynamics. An example of a delay partial differential equation (DPDE) that is used in a furnace to process metal sheets is as follows:

$$
\frac{\partial \hat{w}(s,\tau)}{\partial \tau} - \varepsilon \frac{\partial^2 \hat{w}(s,\tau)}{\partial s^2}
$$
$$
= v(f(\hat{w}(s,\tau-\xi)))\frac{\partial \hat{w}(s,\tau)}{\partial s} + c[g(\hat{w}(s,\tau-\xi)) - \hat{w}(s,\tau)].
$$

For detailed literature on the above delay model, the reader can refer to [32]. DPDEs are closer to real-world phenomena as the solution does not only depend on the solution at a current stage but also at an earlier stage. The highest order derivative of the singularly perturbed delay differential equations (SPPDEs) is multiplied with a small parameter ε, with at least one term included with negative/positive shifts. There are a lot of manuscripts available in the literature dealing with DPDEs. For instance, see [14, 29, 22]. It is challenging to solve the SPPDEs analytically. Additionally, the presence of a small parameter ε leads to a sudden change in solution, resulting

in boundary and interior layers. Moreover, due to the requirements of an unexpectedly large number of mesh points on uniform mesh, a classical numerical method is not practical to accurately capture the layer in the solution. In this sense, the scheme mentioned above fails. So, a singularly perturbed DPDE numerical solution requires special treatment, which leads to the development of a uniform convergent method. Various articles discuss the numerical as well as the analytical aspects of singularly perturbed differential equations via finite difference and finite element methods. For example, see [2, 7, 19, 28, 24, 4, 23, 25]. However, only a few articles are available on partial differential equations with delay arguments in which analytical and numerical solutions are discussed. Ansari, Bakr, and Shishkin [1] used a finite difference method (FDM). Their method is implicit in time and centered in space on a piecewise uniform mesh. They achieved an order of convergence $\mathcal{O}((N^{-1} \ln N)^2 + M^{-1})$ for the singularly perturbed delay parabolic reaction-diffusion problem. Gowrisankar and Natesan [10] solved SPPDEs of a convection-diffusion type by virtue of the FDM. In this article, the spatial domain through the adaptive mesh and temporal variable using implicit Euler has been discretized, and the method converges with order $\mathcal{O}((N^{-1} \ln N) + \Delta t)$. Gowrisankar and Natesan [21] established uniform convergence for a singularly perturbed convection-diffusion problem with a convergence of order $\mathcal{O}(\Delta t + N^{-1+\bar{q}})$, where $0 < \bar{q} < 1$. Kumar and Kumari [15] constructed an ε-uniform convergent FDM for the reaction-diffusion initial-boundary value problem with a delay in the temporal direction. The authors have confirmed the order of convergence for a fully discretized scheme is $\mathcal{O}(\Delta t + N^{-2} \ln^3 N)$ utilizing extended cubic B-spline on the layer-adapted mesh. Kumar et al. [16] have explored uniform convergence of time-delayed parabolic partial differential equations (PDEs) on graded mesh generation algorithms based on entropy function. Das, Govindarao, and Mohapatra [3] proposed a weighted monotone numerical scheme comprised of Crank-Nicolson in time and a weighted monotone hybrid scheme for spatial derivatives on Shishkin mesh, which is parameter uniform converges with order $\mathcal{O}((N^{-1} \ln N)^2 + (\Delta t)^2)$. Gartland [8] studied boundary value problems on the graded mesh in which the scheme converges of order $\mathcal{O}(h^k)$, where k times as many points are available inside the layer as outside. The con-

vergence of order two in both the spatial and temporal variables has been established by Gupta, Kadalbajoo, and Dubey [11]. The difference scheme on the Bakhvalov–Shishkin mesh is used in [12] to explore the first-order convergence. Indeed in all these works, authors have described delay/nondelay problems on layer-adapted mesh only. There are various numerical methods used in different branches of science and engineering; for reference, see [26, 27, 5, 30, 31, 6, 33]. Any work related to the convergence of difference schemes on the modified graded mesh has not been noticed yet. Therefore, we are now in a position to establish a different scheme on the modified graded mesh. Motivated by the work of [1, 10, 4, 23], we proposed an upwind FDM on a modified graded mesh for a time-delayed convection-diffusion parabolic problem. We also establish that the method is almost first-order convergence without a logarithmic factor in the mesh parameter N.

Many articles discuss convection-diffusion problems involving boundary layers with layer adaptive meshes like Shishkin, Bekhvalov, and adaptive meshes. Gowrisankar and Natesan [10] solved SPPDEs of convection-diffusion type by the FDM on piecewise uniform mesh, which converges uniformly with an order $\mathcal{O}((N^{-1}\ln N) + \Delta t)$. Kumar et al. [17] analyzed convection-diffusion problems on the adaptive mesh via equidistribution of monitor function and obtained first-order convergence. Generating adaptive meshes for the parabolic problems requires the iterative process to obtain the grid at each time level. So, it requires high computation in comparison to other meshes discussed above. It is clear from the numerical findings that the modified graded mesh proposed in this work provides the equivalent rate of convergence as the adaptive meshes with negligible computation in comparison with the adaptive algorithm. Also, the modified graded mesh helps improve the accuracy and efficiency of the method.

The description of the problem is as follows: Let $\aleph = \Lambda \times (0, T]$, where $\Lambda = (0, 1)$ and $\Upsilon = \Upsilon_l \cup \Upsilon_b \cup \Upsilon_r$, in which Υ_r and Υ_l are, respectively, the right and left side of the rectangular domain $\aleph$ and $\Upsilon_b = [0, 1] \times [-\xi, 0]$. The following problem on $\aleph = \Lambda \times (0, T]$ is examined in this paper:

$$L_s^\tau \hat{w}(s, \tau) = -\hat{d}(s, \tau)\hat{w}(s, \tau - \xi) + g(s, \tau), \quad \text{for all} \quad (s, \tau) \in \aleph, \quad (1)$$

$$\hat{w}(s, \tau) = \Psi_l(\tau), \quad (s, \tau) \in \{0\} \times \Upsilon_l = \{(0, \tau), 0 < \tau \leq T\},$$

$$\hat{w}(s,\tau) = \Psi_r(\tau), \quad \hat{w}(s,\tau) \in \{1\} \times \Upsilon_r = \{(1,\tau), 0 < \tau \le T\},$$

$$\hat{w}(s,\tau) = \Psi_b(s,\tau), \quad (s,\tau) \in \Upsilon_b = [0,1] \times [-\xi, 0],$$

where

$$L_s^\tau \hat{w}(s,\tau) := \Big(\frac{\partial}{\partial \tau} - \varepsilon \frac{\partial^2}{\partial s^2} + \hat{a}(s,\tau) \frac{\partial}{\partial s} + \hat{b}(s,\tau) \Big) \hat{w}(s,\tau). \tag{2}$$

The above-considered singular perturbation parameter is $\varepsilon \in (0,1]$. Additionally, $\xi \ge 0$, a delay parameter, satisfies the equation $T = q\xi$ for some positive integer q. Here, the above considered functions $\hat{a}(s,\tau)$, $\hat{b}(s,\tau)$, $\hat{d}(s,\tau)$, $g(s,\tau)$, Ψ_b, Ψ_r, Ψ_l, and Ψ_b are sufficiently smooth, bounded and also fulfill the following conditions:

$$\hat{a}(s,\tau) \ge \delta > 0, \quad \hat{b}(s,\tau) \ge 0, \quad \text{and} \quad \hat{d}(s,\tau) \ge \beta > 0.$$

The reduced problem corresponding to (1) is

$$\begin{cases} \frac{\partial \hat{w}_0(s,\tau)}{\partial \tau} + \hat{a}(s,\tau) \frac{\partial \hat{w}_0(s,\tau)}{\partial s} + \hat{b}(s,\tau) \hat{w}_0(s,\tau) \\ \quad = -\hat{d}(x,\tau) \hat{w}_0(s,\tau - \xi) + g(s,\tau), \quad \text{for all} \ (s,\tau) \in \aleph, \\ \hat{w}_0(s,\tau) = \Psi_b(s,\tau), \quad\quad\quad\quad\quad (s,\tau) \in \Upsilon_b = [0,1] \times [-\xi, 0], \\ \hat{w}_0(s,\tau) = \Psi_r(s), \quad\quad\quad\quad\quad\quad (s,\tau) \in \Upsilon_r. \end{cases} \tag{3}$$

By considering s to be constant, the solution to the reduced problem (3) is vertical lines, which ensures that the boundary layer that arises will be of the parabolic type. The compatibility condition for the initial functions $\Psi_b(s,\tau)$ are also satisfied at the corner points $(0,0)$, $(1,0)$, $(0,-\xi)$, and $(1,-\xi)$,

$$\Psi_b(0,0) = \Psi_l(0),$$

$$\Psi_b(1,0) = \Psi_r(0),$$

$$\frac{d\Psi_l(0)}{d\tau} - \varepsilon \frac{\partial^2 \Psi_b(0,0)}{\partial s^2} + \hat{a}(0,0) \frac{\partial \Psi_b(0,0)}{\partial s} + \hat{b}(0,0) \Psi_b(0,0)$$

$$= -\hat{d}(0,0) \Psi_b(0,-\xi) + g(0,0),$$

$$\frac{d\Psi_r(0)}{d\tau} - \varepsilon \frac{\partial^2 \Psi_b(1,0)}{\partial s^2} + \hat{a}(1,0) \frac{\partial \Psi_b(1,0)}{\partial s} + \hat{b}(1,0) \Psi_b(1,0)$$

$$= -\hat{d}(1,0) \Psi_b(1,-\xi) + g(1,0).$$

Notation: Assume that C is used as a generic constant throughout the paper. Also, C is independent of the perturbation parameter ε and the mesh point N. We use discrete maximum norm to study convergence, which is defined as

$$\|\hat{w}\|_\Lambda = \max_{s \in \Lambda} |\hat{w}(s)|.$$

The Paper is presented as follows. Continuous solutions and their derivatives are covered in Section 2. The constructed numerical method is presented in Section 3. Section 4 studies the error analysis of the proposed method. Numerical examples and results support the theoretical findings in Section 5. The paper ends with a conclusion presented in Section 6.

2 Bounds for continuous solution and its derivatives

This section discusses the bounds for the solution and its partial derivatives across the prescribed domain. Furthermore, for the proof of ε-uniform convergence in a later section, we split the analytical solution $\hat{w}$ of (1). Also, it establishes strong bounds on the layer and smooth component, which we obtain by splitting the analytical solution. The operator L_s^τ defined in (2) satisfies the following maximum principle.

Lemma 1 (Maximum principle). [15] Assume that $\xi(s, \tau) \geq 0$ holds true for all values of $(s, \tau) \in \Upsilon$. If $L_s^\tau \xi(s, \tau) \geq 0$ for all $(s, \tau) \in \aleph$, then $\xi(s, \tau) \geq 0$ for all $(s, \tau) \in \overline{\aleph}$.

Proof. Suppose $(s^*, \tau^*) \in \overline{\aleph}$ such that

$$\xi(s^*, \tau^*) = \min \xi(s, \tau),$$

and assume $\xi(s^*, \tau^*) < 0$. Also, we have $\frac{\partial \xi(s^*, \tau^*)}{\partial s} = 0$, $\frac{\partial \xi(s^*, \tau^*)}{\partial \tau} = 0$, and $\frac{\partial^2 \xi(s^*, \tau^*)}{\partial \tau^2} \geq 0$. Then

$$L_s^\tau \xi(s^*, \tau^*) < 0,$$

which is contrary to our supposition. It follows that $\xi(s^*, \tau^*) \geq 0$ and so $\xi(s, \tau) \geq 0$ for all $(s, \tau) \in \overline{\aleph}$. $\square$

Lemma 2 (Uniform stability bounds). [13, 1] For the specified function η in the defined domain of the differential operator L_s^τ in (2), we have

$$\|\eta\| \le (1 + \alpha T) \max\{\|L_s^\tau \eta\|, \|\eta_l\|, \|\eta_r\|, \|\eta_b\|\},$$

and for any solution $\hat{w}(s, \tau)$ of (1), we have

$$\|\hat{w}(s, \tau)\| \le (1 + \alpha T) \max\{\|g\|, \|\Psi_l\|, \|\Psi_r\|, \|\Psi_b\|\},$$

where $\alpha = \max\{0, 1 - \delta\}$.

Proof. We define barrier function as

$$\psi^\pm(s, \tau) = (1 + \alpha T) \max\{\|g\|, \|\Psi_l(\tau)\|, \|\Psi_r(\tau)\|, \|\Psi_b(\tau)\|\} \pm \hat{w}(s, \tau),$$
$$\text{for all } (s, \tau) \in \overline{\aleph}.$$

Then, at initial condition

$$\psi^\pm(s, 0) = (1 + \alpha T) \max\{\|g\|, \|\Psi_l(0)\|, \|\Psi_r(0)\|, \|\Psi_b(0)\|\} \pm \hat{w}(s, 0),$$

we obtain

$$\psi^\pm(s, 0) \ge 0, \quad \text{for all } (s, \tau) \in \Upsilon_b.$$

At boundary points, we have

$$\psi^\pm(0, \tau) = (1 + \alpha T) \max\{\|g\|, \|\Psi_l(\tau)\|, \|\Psi_r(\tau)\|, \|\Psi_b(\tau)\|\} \pm \hat{w}(0, \tau),$$

which gives

$$\psi^\pm(0, \tau) \ge 0, \quad \text{for all } (s, \tau) \in \Upsilon_l.$$

Similarly, we have

$$\psi^\pm(1, \tau) \ge 0, \quad \text{for all } (s, \tau) \in \Upsilon_r.$$

The differential operator L_s^τ satisfies

$$L_s^\tau \psi^\pm(s, \tau) = (\pm \hat{w}_\tau(s, \tau) - \varepsilon(\pm \hat{w}_{ss}(s, \tau)) + \hat{a}(s, \tau)(\pm \hat{w}_s(s, \tau)),$$
$$+ \hat{b}(s, \tau)((1 + \alpha T) \max\{\|g\|, \|\Psi_l(\tau)\|, \|\Psi_r(\tau)\|, \|\Psi_b(\tau)\|\} \pm \hat{w}(s, \tau)))$$
$$= (\pm \hat{w}_\tau(s, \tau) \mp \varepsilon(\hat{w}_{ss}(s, \tau)) \pm \hat{a}(s, \tau)\hat{w}_s(s, \tau) \pm \hat{b}(s, \tau)\hat{w}(s, \tau),$$
$$+ \hat{b}(s, \tau)((1 + \alpha T) \max\{\|g\|, \|\Psi_l(\tau)\|, \|\Psi_r(\tau)\|, \|\Psi_b(\tau)\|\} \pm \hat{w}(s, \tau)))$$
$$= L_s^\tau \hat{w}(s, \tau) + \hat{b}(s, \tau)((1 + \alpha T) \max \|g\|, \|\Psi_l(\tau)\|, \|\Psi_r(\tau)\|, \|\Psi_b(\tau)\|)$$
$$\ge 0.$$

Thus, the maximum principle asserts that

$$\psi^{\pm}(s,\tau) \geq 0, \quad \text{for all} \ \ (s,\tau) \ \in \overline{\aleph}.$$

Finally, we get

$$\|\hat{w}(s,\tau)\| \leq (1 + \alpha T) \max\{\|g\|, \|\Psi_l\|, \|\Psi_r\|, \|\Psi_b\|\}.$$

$\square$

Theorem 1. Let the data $\hat{a} \in C^{(2+\gamma,1+\gamma/2)}(\overline{\Lambda})$, $\hat{b}$, $\hat{d}$, $g \in C^{(2+\gamma,1+\gamma/2)}$ $(\overline{\aleph})$, $\Psi_l \in C^{2+\gamma/2}([0,T])$, $\Psi_r \in C^{2+\gamma/2}([0,T])$, $\Psi_b \in C^{(4+\gamma,2+\gamma/2)}(\Upsilon_b)$, $\gamma \in (0,1)$, meet the necessary compatibility requirement on the corner. Consequently, (1) has a unique solution $\hat{w}$ and $\hat{w} \in C^{(4+\gamma,2+\gamma/2)}$ $(\overline{\aleph})$. Additionally, bounds on derivatives of solution $\hat{w}(s,\tau)$ is satisfied for all nonnegative integers i and j, where $0 \leq i + 2j \leq 4$,

$$\left\| \frac{\partial^{i+j}\hat{w}}{\partial s^i \partial \tau^j} \right\| \leq C\varepsilon^{-i}.$$

Proof. The proof of existence and uniqueness can be found in [18]. To establish the derivative bound, the variable s is replaced to $\varepsilon\vartheta = s$ and follows the approach given in [1]. $\square$

In the above Theorem 1, we establish the bound for exact solution $\hat{w}(s,\tau)$, which is not sufficient to establish the ε-uniform convergence of the method. In order to get strong bounds on the derivatives of the exact solution $\hat{w}$, we decompose the above $\hat{w}$ into smooth and layer component,

$$\hat{w}(s,\tau) = \hat{v}(s,\tau) + w(s,\tau), \quad (s,\tau) \in \overline{\aleph},$$

where the following differential equations are satisfied by the smooth component, $\hat{v}(s,\tau)$,

$$L_s^\tau \hat{v}(s,\tau) = -\hat{d}(s,\tau)\hat{v}(s,\tau - \xi) + g(s,\tau), \quad (s,\tau) \in \aleph,$$

with initial condition

$$\hat{v}(s,\tau) = \hat{w}(s,\tau), \quad (s,\tau) \in \Upsilon_b,$$

and the boundary condition

$$\hat{v}(0,\tau) = \hat{w}(0,\tau), \ \hat{v}(1,\tau) = \hat{w}(1,\tau), \quad 0 \leq \tau \leq T.$$

The smooth component $\hat{v}(s,\tau)$ is further decomposed as

$$\hat{v}(s,\tau) = \hat{v}_0(s,\tau) + \varepsilon\hat{v}_1(s,\tau), \qquad (s,\tau) \in \bar{\aleph},$$

where $\hat{v}_0(s,\tau)$ is the solution of reduced problem

$$\frac{\partial\hat{v}_0(s,\tau)}{\partial\tau} + \hat{a}(s,\tau)\frac{\partial\hat{v}_0(s,\tau)}{\partial s} + \hat{b}(s,\tau)\hat{v}_0(s,\tau)$$
$$= -\hat{d}(s,\tau)\hat{v}_0(s,\tau-\xi) + g(s,\tau), \quad \text{for all } (s,\tau) \in \aleph,$$
$$\hat{v}_0(s,\tau) = \Psi_b(s,\tau), \qquad (s,\tau) \in \Upsilon_b,$$

and $\hat{v}_1(s,\tau)$ satisfies the following problem,

$$\frac{\partial\hat{v}_1(s,\tau)}{\partial\tau} + \hat{a}(s,\tau)\frac{\partial\hat{v}_1(s,\tau)}{\partial s} + \hat{b}(s,\tau)\hat{v}_1(s,\tau)$$
$$= -\hat{d}(s,\tau)\hat{v}_1(s,\tau-\xi) + \frac{\partial^2\hat{v}_0(s,\tau)}{\partial s^2}, \quad (s,\tau) \in \aleph,$$
$$\hat{v}_1(s,\tau) = 0, \quad (s,\tau) \in \Upsilon_b.$$

Furthermore, $\hat{v}$ satisfies

$$L_s^\tau\hat{v}(s,\tau) = -\hat{d}(s,\tau)\hat{v}(s,\tau-\tau) + g(s,\tau), \qquad (s,\tau) \in \aleph,$$
$$\hat{v}(s,\tau) = \hat{w}(s,\tau), \qquad (s,\tau) \in \Upsilon_b,$$
$$\hat{v}(0,\tau) = \hat{v}_0(0,\tau), \quad \hat{v}(1,\tau) = \hat{v}_0(1,\tau) + \varepsilon\hat{v}_1(1,\tau), \qquad \tau \in [0,T],$$

and the singular components w satisfies

$$L_s^\tau w(s,\tau) = -\hat{d}w(s,\tau-\xi), \qquad (s,\tau) \in \aleph,$$
$$w(s,\tau) = 0, \qquad (s,\tau) \in \Upsilon_b,$$
$$w(0,\tau) = 0, \qquad w(1,\tau) = \hat{w}(1,\tau) - \hat{v}(1,\tau), \qquad \tau \in [0,T],$$

and the estimation of singular and the smooth component are discussed in Theorem 2 given below.

Theorem 2. Assume that $\hat{a} \in C^{(4+\gamma,2+\gamma/2)}(\bar{\Lambda})$, $\hat{b},\hat{d},g \in C^{(4+\gamma,2+\gamma/2)}(\bar{\aleph})$, $\Psi_l \in C^{3+\gamma/2}([0,T])$, $\Psi_r \in C^{3+\gamma/2}([0,T])$, $\Psi_b \in C^{(6+\gamma,3+\gamma/2)}(\Upsilon_b)$, $\gamma \in (0,1)$, fulfill the necessary compatibility condition on the corner. Then, for all nonnegative integers i,j such that $0 \le i+2j \le 4$, we have the following bounds for the smooth $\hat{v}$ and the layer part w in the decomposition of solution $\hat{w}$ is

$$\left\| \frac{\partial^{i+j} \hat{v}}{\partial s^i \partial \tau^j} \right\| \le C(1 + \varepsilon^{1-i}),$$

and

$$\left\| \frac{\partial^{i+j} w}{\partial s^i \partial \tau^j} \right\| \le C\varepsilon^{-i} e^{-\gamma s/\varepsilon}.$$

Proof. For the proof of theorem, one may refer [20]. □

3 Grid construction and numerical discretization

In this section, grids are developed to discretize the problem in both spatial and temporal directions. Later, we use a backward Euler in the temporal direction and an upwind method on the spatial derivative for the discretization of the problem (1).

3.1 Temporal discretization

To establish the convergence of (1) at each instance, we use the uniform time grid.

$$\Omega^M = \{\tau_k = k\Delta\tau, \quad k = 0, \ 1, \ \ldots, \ M, \quad \Delta\tau M = T\}.$$

Here M represents the grid points in the temporal direction.

3.2 Spatial discretization

We generate a modified graded mesh, Λ_s^N in the interval $[0,1]$ as follows:

$$\begin{cases} \mu_0 = 0, \\ \mu_j = 2\varepsilon \frac{j}{N}, & 1 \le j \le \frac{N}{2}, \\ \mu_{j+1} = \mu_j(1 + \rho h), & \frac{N}{2} \le j \le N - 2, \\ \mu_N = 1, \end{cases} \tag{4}$$

where the parameter h satisfies the following nonlinear equation:

$$\ln(1/\varepsilon) = (N/2)\ln(1 + \rho h). \tag{5}$$

The above selection of the parameter h ensures that there are $N/2$ grid points in the interval $[\varepsilon, 1]$, which are distributed gradely in the interval $[\varepsilon, 1]$. Numerical verification stimulates that in comparison to (μ_{N-2}, μ_{N-1}), the interval $(\mu_{N-1}, 1)$ is not too small. In the subinterval $[0, \varepsilon]$, we distribute $N/2$ points with uniform step length $2\varepsilon/N$, while in the subinterval $[\varepsilon, 1]$, we first find h for some fix N by means of the nonlinear equation (5), and corresponding to that h, we distribute $N/2$ points in $[\varepsilon, 1]$.

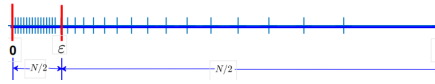The mesh length is denoted by $h_j = \mu_j - \mu_{j-1}$ for $j = 1, 2, \ldots, N$.

Figure 1: Modified graded mesh for $N = 32$ and $\varepsilon = 10^{-1}$.

Remark 1. The mesh size in piecewise uniform and the modified graded region is given by

$$h_j = \begin{cases} 2\varepsilon/N & \text{for } j = 1,\ 2,\ \ldots,\ N/2, \\ \rho h \mu_{j-1} & \text{for } j = N/2+1,\ N/2+2,\ \ldots,\ N. \end{cases}$$

Lemma 3. The mesh defined in (4) satisfies the following estimates:

$$|h_{j+1} - h_j| \le \begin{cases} 0 & for\ j = 1,\ 2,\ \ldots,\ N/2, \\ Ch & for\ j = N/2+1,\ N/2+2,\ \ldots,\ N. \end{cases}$$

Proof. Initially, we consider $j = 1,\ 2,\ \ldots,\ N/2$. As the mesh is uniform in this portion, so nothing to prove.

For $j = N/2+1,\ N/2+2,\ \ldots,\ N$. We have

$$\begin{aligned} |h_{j+1} - h_j| &= |\rho h \mu_j - \rho h \mu_{j-1}| \\ &= \rho h |\mu_j - \mu_{j-1}| \\ &= \rho^2 h^2 \mu_{j-1} \\ &\le Ch. \end{aligned}$$

Here, we have taken $0 < \rho, h < 1$. $\qquad\qquad\qquad\qquad\qquad\qquad \square$

Lemma 4. For the modified graded mesh defined in (4), the parameter h satisfies the following bound,

$$h \leq CN^{-1} \ln(1/\varepsilon).$$

Proof. Let K_1 denote the number of partitioned points in (4) such that $\mu_j \leq \varepsilon$, for $j = 1, 2, \ldots, N/2$. Clearly, $K_1 \leq C/h$. Let K_2 be the number of points in the partition (4) such that $\mu_j > \varepsilon$. Let $\mu_{N/2+1}$ be the smallest point such that $\mu_j > \varepsilon$. We have to estimate the bound for K_2. Assuming $\rho h \leq 1$, we have

$$
\begin{aligned}
K_2 &= \sum_{N/2+1}^{N} 1 = \sum_{N/2+1}^{N} (\mu_{j+1} - \mu_j)^{-1} \int_{\mu_j}^{\mu_{j+1}} d\mu \\
&= \sum_{N/2+1}^{N} (h_{j+1})^{-1} \int_{\mu_j}^{\mu_{j+1}} d\mu \\
&= \sum_{N/2+1}^{N} (h\rho\mu_j)^{-1} \int_{\mu_j}^{\mu_{j+1}} d\mu \\
&\leq \sum_{N/2+1}^{N} (2/\rho h\mu_{j+1})^{-1} \int_{\mu_j}^{\mu_{j+1}} d\mu,
\end{aligned}
$$

because $\mu_{j+1} < 2\mu_j$. For any $\mu \in [\mu_j, \mu_{j+1}]$, we have

$$
\begin{aligned}
K_2 &\leq \sum_{N/2+1}^{N} 2(\rho h)^{-1} \int_{\mu_j}^{\mu_{j+1}} \frac{1}{\mu} d\mu \\
&\leq 2(\rho h)^{-1} \int_{\varepsilon}^{1} \frac{1}{\mu} d\mu \\
&\leq 2(\rho h)^{-1} \ln(1/\varepsilon).
\end{aligned}
$$

Recalling $N = K_1 + K_2$, we have

$$
\begin{aligned}
N &\leq C/\rho h + 2(\rho h)^{-1} \ln(1/\varepsilon) \\
N &\leq 1/h(\rho C + 2\rho \ln(1/\varepsilon)) \\
N &\leq 1/h(C \ln(1/\varepsilon)).
\end{aligned}
$$

Finally, we get

$$h \leq CN^{-1} \ln(1/\varepsilon),$$

where N represents grid points in the s-direction.   □

Now, we systematically discretize our domain. For this, a non-uniform grid Λ_s^N on Λ with N mesh points is obtained by distributing $N/2$ points uniformly in the layer part and $N/2$ points nonuniformly outside the layer part. Here, we consider an equidistant grid Ω^M and Ω^l with uniform step-length $\Delta\tau$ on $[0, T]$ and $[-\xi, 0]$ with M and l grid points, respectively. Then, the discretized domain will define as

$$\aleph^N = \Lambda_s^N \times \Omega^M, \quad \Upsilon_b^N = \Lambda_s^N \times \Omega^l,$$

and the boundary points Υ^N of $\aleph^N$ are $\Upsilon^N = \bar{\aleph}^N \cap \Upsilon$. Additionally, Υ_l^N $= \aleph^N \cap \Upsilon_l$ and $\Upsilon_r^N = \aleph^N \cap \Upsilon_r$ define the left and right boundary points, respectively. Also, $\aleph_i^N = \Lambda_s^N \times \Omega_{i,\tau}^l$, where $\Omega_{i,\tau}^l$ is the set of uniform mesh in $[(i-1)\xi, i\xi]$. Now, we discretize our problem with the above-discretized mesh. We apply an upwind difference method and backward Euler for spatial and temporal derivatives. Then

$$\begin{cases} (D_\tau^- - \varepsilon\frac{D_s^+ - D_s^-}{\widehat{h}_j} + \hat{a}(j, k+1) \ D_s^+)S_{j,k+1} \\ \qquad + \hat{b}_{j,k+1}S_{j,k+1} = -\hat{d}(j, k+1)S_{j,k-l} + g_{j,k+1}, \\ S_{0,k+1} = \Psi_l(\tau_{k+1}), \\ S_{N,k+1} = \Psi_r(\tau_{k+1}), \\ S_{j,-p} = \Psi_b(s_j, -\tau_p), \qquad j = 1, \ 2, \ \ldots, \ N-1, \ p = 0, \ 1, \ \ldots, \ l. \end{cases} \quad (6)$$

By arranging (6), we will get a tri-diagonal system

$$(\alpha_{j,k+1})S_{j-1,k+1} + (\beta_{j,k+1})S_{j,k+1} + (\gamma_{j,k+1})S_{j+1,k+1} = h_{j,k}, \quad (7)$$

where

$$\alpha_{j,k+1} = \frac{-\varepsilon\Delta\tau}{h_j\hat{h}_j},$$

$$\beta_{j,k+1} = 1 + \frac{\varepsilon\Delta\tau}{h_{j+1}\hat{h}_j} + \frac{\varepsilon\Delta\tau}{h_j\hat{h}_j} - \frac{\hat{a}(j, k+1)\Delta\tau}{h_{j+1}} + \hat{b}_{j,k+1}\Delta\tau,$$

$$\gamma_{j,k+1} = \frac{-\varepsilon\Delta\tau}{h_{j+1}\hat{h}_j} + \frac{a(j, k+1)\Delta\tau}{h_{j+1}},$$

$$h_{j,k} = -\hat{d}(j, k+1)S_{j,k-l}\Delta\tau + g_{j,k+1}\Delta\tau + S_{j,k},$$

$$\hat{h}_j = \frac{h_{j+1} + h_j}{2},$$

and the step length $\Delta\tau$ satisfies $l\Delta\tau = \xi$, and also $\tau_p = p\Delta\tau$, $p \geq -l$, and l is a positive integer and the mesh function $\widetilde{v}(s_j, \tau_k) = \widetilde{v}_{j,k}$ is defined by

$$D_s^+\widetilde{v}_{j,k} = \frac{\widetilde{v}_{j+1,k} - \widetilde{v}_{j,k}}{h_{j+1}}, \quad D_s^-\widetilde{v}_{j,k} = \frac{\widetilde{v}_{j,k} - \widetilde{v}_{j-1,k}}{h_j},$$

$$D_\tau^-\widetilde{v}_{j,k} = \frac{\widetilde{v}_{j,k} - \widetilde{v}_{j,k-1}}{h_{j+1}},$$

and

$$\delta_s^2\widetilde{v}_{j,k} = \frac{(D_s^+ - D_s^-)\widetilde{v}_{j,k}}{\hat{h}_j}.$$

3.3 Numerical algorithm

The following algorithm provides the grid construction and the corresponding numerical solution:

Step 1. Given the number of mesh points in the temporal and the spatial direction, M and N, respectively, take uniform mesh points in the temporal direction, $\{\tau_k\}_{k=0}^M$.

Step 2. For the finer part in the spatial direction (i.e., $[0, \varepsilon]$), we have the uniform mesh $\{\mu_j\}_{j=0}^{N/2}$.

Step 3. For the coarser part (i.e., $[\varepsilon, 1]$), the graded mesh parameter h is obtained by solving the nonlinear equation (5) by the bisection method.

Step 4. Using the graded mesh parameter h, obtain the graded mesh in the interval $[\varepsilon, 1]$ from (4).

Step 5. Set $k = 1$.

Step 6. For the value of k, solve the tridiagonal system (7) to obtain the solution for the time level $t = k$.

Step 7. $k = k + 1$ goto Step 6.

Step 8. If $k = M$, then stop and mark $S_{j,k}$, as the required solution.

4 Error analysis

Lemma 5 (Discrete maximum principle)**.** [9] Assume that the mesh function $\xi(s_j, \tau_k)$ satisfies $\xi(s_j, \tau_k) \geq 0$ on Υ^N. If $L_s^{\tau,N} \xi(s_j, \tau_k) \geq 0$ on $(s_j, \tau_k) \in \aleph^N$, then $\xi(s_j, \tau_k) \geq 0$ on $\overline{\aleph}^N$.

Lemma 6. For any solution $S(s_j, \tau_k)$ of (6), we have

$$\|S(s_j, \tau_k)\| \leq (1 + \alpha T) \max(\|L_s^{\tau,N}\|\|, \|\Psi\|_{\Upsilon^N}). \tag{8}$$

Proof. By constructing the barrier function, we have

$$\hat{S}^\pm(s_j, \tau_k) = (1 + \alpha T) \max(\|L_s^{\tau,N}\|\|, \|\Psi\|_{\Upsilon^N}) \pm S(s_j, \tau_k). \tag{9}$$

We can obtain (8) by applying (5) on (9).   □

Theorem 3. Let $\hat{w}$ and S be the solution of continuous problem (1) and discretized problem (6), respectively. Furthermore, the both solutions meet the corners compatibility requirements. Then, the error estimate is given by

$$\max |(\hat{w} - S)(s_j, \tau_k)| \leq C[\Delta\tau + N^{-1} \ln(1/\varepsilon)], \quad (s_j, \tau_k) \in \aleph^N. \tag{10}$$

Here, constant C is free from N, $\Delta\tau$, and ε.

Proof. The proof is similar to the proof given in [10, 1]. We derive it by using our mesh briefed in sections 3.1 and 3.2 and (5).

To prove the theorem for different time levels, we first divide the domain $\aleph$ into $\aleph = \aleph_1 \cup \aleph_2$, where $\aleph_1 = \Lambda \times [0, \xi]$ and $\aleph_2 = \Lambda \times [\xi, 2\xi]$. The discretized domain $\aleph^N = \aleph_1^N \times \aleph_2^N$, where $\aleph_1^N = \Lambda_s^N \times \Omega^l$ and $\aleph_2^N = \Lambda_s^N \times \Omega^M$.

First, for $\tau \in [0, \xi]$, the right-hand side of (1) becomes $-\hat{d}(s, \tau)\hat{w}(s, \tau - \xi) + g(s, \tau)$, which is free from ε. Thus the results in [10] is applicable, and we obtain

$$\max |(\hat{w} - S)(s_j, \tau_k)| \leq C[\Delta\tau + N^{-1} \ln(1/\varepsilon)]. \tag{11}$$

For $\tau \geq \xi$, the term $\hat{w}(s, \tau - \xi)$ is not free from ε. So, we are required to examine the estimates between the numerical solution S and the analytical solution $\hat{w}$ over the interval $[\xi, 2\xi]$. The following SPPDEs is considered:

$$\Big(\frac{\partial}{\partial \tau} - \varepsilon \frac{\partial^2}{\partial s^2} + \hat{a}(s, \tau)\frac{\partial}{\partial s} + \hat{b}(s, \tau) \Big)\hat{w}(s, \tau)$$

$$= -\hat{d}(s,\tau)\hat{w}(s,\tau-\xi) + g(s,\tau), \quad (s,\tau) \in \aleph_2^N, \qquad (12)$$

$$\hat{w}(s,\tau) = \hat{w}(s,\tau_l), \quad s \in (0,1),$$

$$\hat{w}(0,t) = \Psi_0(\tau), \quad \hat{w}(1,\tau) = \Psi_1(\tau), \quad \tau \in [\xi, 2\xi].$$

To determine the numerical solution, we discretize (12) by using upwind finite difference for spatial derivatives and the backward-Euler for time derivative,

$$L_s^\tau S(s_j,\tau_k) \equiv D_\tau^- S_{j,k} - \varepsilon \delta_s^2 S_{j,k} + \hat{a}_{j,k} D_s^- Sj, k + \hat{b}_{j,k} S_{j,k}$$

$$= -\hat{d}_{j,k} S_{j,k-l} + g(s_j,\tau_k), \quad (s_j,\tau_k) \in \aleph_2^N, \qquad (13)$$

$$S(s_j,\tau_k) = S_1(s_j,\tau_k), \quad (s_j,\tau_k) \in \aleph^N,$$

$$S(0,\tau_k) = \Psi_0(\tau_k),$$

$$S(1,\tau_k) = \Psi_1(\tau_k), \quad \tau_k \in \Omega_{2,\tau}^l,$$

where $S_1(s_j,\tau_k)$ is the approximate solution obtained over the interval $\aleph_1^N$. Now, we divide the solution $\hat{w}$ of (1) into its regular and singular components as $\hat{w} = \hat{y} + \hat{z}$, and furthermore, $\hat{y} = y_0 + \varepsilon y_1$, where y_0 is the solution to the reduced problem,

$$\left(\frac{\partial}{\partial \tau} + \hat{a}(s,\tau)\frac{\partial}{\partial s} + \hat{b}(s,\tau)\right) y_0(s,\tau)$$

$$= -\hat{d}y_0(s,\tau-\xi) + g(s,\tau), \quad (s,\tau) \in (0,1) \times (\xi, 2\xi),$$

$$y_0(s,\tau) = \hat{w}(s,\tau), \quad (s,\tau) \in (0,1) \times [0,\xi],$$

$$y_0(0,\tau) = \hat{w}(0,\tau), \quad \tau \in [\xi, 2\xi],$$

and

$$L_s^\tau y_1(s,\tau) = -\hat{d}(s,\tau) y_1(s,\tau-\xi) + \frac{\partial^2 y_0(s,\tau)}{\partial s^2},$$

$$y_1(s,\tau) = 0, \quad (s,\tau) \in (0,1) \times [0,\xi],$$

$$y_1(0,\tau) = y_1(1,\tau) = 0, \quad \tau \in [\xi, 2\xi].$$

Furthermore, $\hat{y}$ satisfies

$$L_s^\tau \hat{y}(s,\tau) = -\hat{d}(s,\tau)\hat{y}(s,\tau-\xi) + g(s,\tau), \quad (s,\tau) \in (0,1) \times [\xi,\xi],$$

$$\hat{y}(s,\tau) = \hat{w}(s,\tau), \quad (s,\tau) \in (0,1) \times [0,\xi],$$

$$\hat{y}(0,\tau) = y_0(0,\tau), \quad \hat{y}(1,\tau) = y_0(1,\tau), \quad \tau \in [\xi, 2\xi].$$

The singular components z satisfies

$$L_s^\tau \hat{z}(s, \tau - \xi) = -\hat{d}\hat{z}(s, \tau - \xi), \quad (s, \tau) \in (0, 1) \times (\xi, 2\xi),$$

$$\hat{z}(s, \tau) = 0, \quad (s, \tau) \in (0, 1) \times [0, \xi],$$

$$\hat{z}(1, \tau) = 0, \quad \hat{z}(0, \tau) = \Psi_l(\tau) - y_0(0, \tau), \quad \tau \in [\xi, 2\xi].$$

Now, we decompose the numerical solution S of (13) into $S = Y + Z$. Here, Z represents the singular component of the decomposition, and Y, the regular component, is the solution to the following non-homogeneous problem:

$$L_s^{\tau,N} Y = -\hat{d}Y(s_j, \tau_{k-l}) + g(s_j, \tau_k), \quad (s_j, \tau_k) \in \aleph_2^N,$$

$$Y(s_j, \tau_k) = S_1(s_j, \tau_k), \quad (s_j, \tau_k) \in (0, 1) \times (0, \xi),$$

$$Y(0, \tau_k) = \hat{y}(0, \tau_k), \quad Y(1, \tau_k) = \hat{y}(1, \tau_k), \quad \tau_k \in \Omega_{2,\tau}^l,$$

and the singular component Z must satisfy

$$L_s^{\tau,N} Z = -\hat{d}Z(s_j, \tau_{k-l}), \quad (s_j, \tau_k) \in \aleph_2^N,$$

$$Z(s_j, \tau_k) = 0, \quad (s_j, \tau_k) \in \aleph_1^N,$$

$$Z(1, \tau_k) = 0, \quad Z(0, \tau_k) = \Psi_l(\tau_k) - \hat{y}(0, \tau_k), \quad \tau_k \in \Omega_{2,\tau}^l.$$

Therefore, the error can be written in the form

$$S - \hat{w} = (Y - \hat{y}) + (Z - \hat{z}).$$

Now, we will establish the bounds for the smooth and the layer components. To establish the bound for the smooth component, we use the classical argument. The smooth error component can be expressed as

$$L_s^{\tau,N}(Y - \hat{y}) = -\hat{d}Y(s_j, \tau_{k-l}) + g(s_j, \tau_k) - L_s^{\tau,N}\hat{y}$$

$$= -\hat{d}Y(s_j, \tau_{k-l}) + L_s^\tau \hat{y} + \hat{d}\hat{y}(s_j, \tau_{k-l}) - L_s^{\tau,N}\hat{y}$$

$$= \hat{d}(\hat{y}(s_j, \tau_{k-l}) - Y(s_j, \tau_{k-l})) + L_s^{\tau,N}\hat{y}.$$

Thus we obtain

$$L_s^{\tau,N}(Y - \hat{y}) = \hat{d}(\hat{y}(s_j, \tau_{k-l}) - Y(s_j, \tau_{k-l})) - \varepsilon(\frac{\partial^2}{\partial s^2} - \delta_s^2)\hat{y}$$

$$+ (\frac{\partial}{\partial \tau} - \delta_\tau)\hat{y} + \hat{a}(s_j, \tau_k)(\frac{\partial}{\partial s} - \delta_s^-)\hat{y}.$$

When absolute values are taken on both sides and used with (10), the above inequality becomes

$$|L_s^{\tau,N}(Y-\hat{y})| \le C(\Delta\tau + N^{-1}\ln(1/\varepsilon)) + \varepsilon|(\frac{\partial^2}{\partial s^2} - \delta_s^2)\hat{y}|$$
$$+ |(\frac{\partial}{\partial s} - \delta_s^-)\hat{y}| + |(\frac{\partial}{\partial\tau} - \delta_\tau)\hat{y}|.$$

Using the Taylor series expansion, we have

$$|L_s^{\tau,N}(Y-\hat{y})| \le C(\Delta\tau + N^{-1}\ln(1/\varepsilon)) + \frac{\varepsilon}{12}(s_{j+1}-s_{j-1})^2\left\|\frac{\partial^4\hat{y}}{\partial s^4}\right\|$$
$$+ (s_j-s_{j-1})\left\|\frac{\partial^2\hat{y}}{\partial s^2}\right\| + \frac{(\tau_k-\tau_{k-1})}{2}\left\|\frac{\partial^2\hat{y}}{\partial\tau^2}\right\|.$$

On using the estimates of derivatives, bounds of mesh length, and discrete maximum principle, we have

$$|(Y-\hat{y})(s_j,\tau_k)| \le C[\Delta\tau + N^{-1}\ln(1/\varepsilon)]. \tag{14}$$

Like continuous z, Z is discretized for estimating the singular component. Thus

$$L_s^{\tau,N}Z = -\hat{d}Z(s_j,\tau_{k-l}), \quad (s_j,\tau_k) \in \aleph_2^N,$$
$$Z(s_j,\tau_k) = 0, \quad (s_j,\tau_k) \in \aleph_2^N,$$
$$Z(1,\tau_k) = 0, \quad Z(0,\tau_k) = \Psi_l(\tau_k) - \hat{y}(0,\tau_k), \quad \tau_k \in \Omega_{2,\tau}^l.$$

The singular component error can be expressed as

$$L_s^{\tau,N}(Z-\hat{z}) = L_s^{\tau,N}Z - L_s^{\tau,N}\hat{z}$$
$$= -\hat{d}Z(s_i,\tau_{n-l}) - L_s^{\tau,N}\hat{z}$$
$$= (L_s^\tau - L_s^{\tau,N})\hat{z}$$
$$= -\varepsilon(\frac{\partial^2}{\partial s^2} - \delta_s^2)\hat{z} + (\frac{\partial}{\partial\tau} - \delta_\tau)\hat{z}.$$

Then, the classical estimates gives

$$|L_s^{\tau,N}(Z-\hat{z})(s_j,\tau_k)| \le C[\Delta\tau + N^{-1}\ln(1/\varepsilon)].$$

The discrete maximum principle is satisfied by the operator $L_s^{\tau,N}$ and also, due to the uniform boundedness of the inverse operator, the above inequality

reduces to

$$|(Z - \hat{z})(s_j, \tau_k)| \leq C[\Delta\tau + N^{-1}\ln(1/\varepsilon)]. \tag{15}$$

Combining (14) and (15) completes the proof on $[\xi, 2\xi]$. In the similar fashion, we estimate the error in the successive interval in time by using induction. $\square$

5 The numerical result with examples

This section consists of two test examples with boundary layers to illustrate the numerical method discussed above. Using tables and graphs, we present the findings of numerical methods. All the results are performed by taking $\rho = 0.9$. Numerical results confirm our theoretical findings.

Example 1. Consider the following problem:

$$\begin{cases} \hat{w}_\tau(s,\tau) - \varepsilon\hat{w}_{ss}(s,\tau) - \hat{w}_s(s,\tau) \\ \quad = \hat{w}(s, \tau-1) + g(s,\tau), & (s,\tau) \in (0,1) \times (0,2], \\ \hat{w}(s,0) = \hat{w}_0(s,\tau), & (s,\tau) \in (0,1) \times [-1,0], \\ \hat{w}(0,\tau) = \tau, & \hat{w}(1,\tau) = 0, \quad \tau \in [0,2]. \end{cases}$$

Using the exact solution, $\hat{w}(s,\tau) = \frac{e^{-s/\varepsilon} - e^{-1/\varepsilon}}{1 - e^{-1/\varepsilon}}\tau + 2\tau s\cos((\pi s)/2)$, we will obtain $\hat{w}_0(s,\tau)$ and $g(s,\tau)$. Additionally, the maximum point-wise error for each ε is defined by

$$e_\varepsilon^{N,\Delta\tau} = \max|(\hat{w} - S)(s_j, \tau_k)| \quad (s_j, \tau_k) \in \aleph^N,$$

where $\hat{w}$ and S are exact and approximate solution, respectively. The order of convergence is computed by

$$p_\varepsilon^{N,\Delta\tau} = \frac{\log(e^{N,\Delta\tau}/e^{2N,\Delta\tau/2})}{\log 2}.$$

For Example 1, the computed maximum pointwise error in the layer region is shown in Table 1, and the associated convergence order is in Table 2. Additionally, in the smooth region, Table 3 shows the maximum pointwise error, and Table 4 presents the related order of convergence. The plots for the numerical solution of Example 1 for the parameters $N = 128$, $\varepsilon = 10^{-2}$

and $\varepsilon = 10^{-8}$ are shown in Figures 2a and 2b. At $s = 0$, the figure shows the existence of a boundary layer. Error plot of Example 1 for $N = 128$, $\varepsilon = 10^{-2}$, and $\varepsilon = 10^{-8}$ is presented in Figure 3a and 3b, respectively. Figure 6a is a plot of Example 1 on the log-log scale for maximum pointwise error. From Table 5 and Figure 6a, it is clear that the applied scheme is first-order uniformly convergent.

Table 1: Maximum error on the modified graded mesh in the layer region for Example 1

ε	Number of intervals $N/\Delta\tau$
	$128/\frac{1}{10}$	$256/\frac{1}{20}$	$512/\frac{1}{40}$	$1024/\frac{1}{80}$	$2048/\frac{1}{160}$	$4096/\frac{1}{320}$
10^{-2}	2.2150E-01	1.0252E-01	4.8929E-02	2.3896E-02	1.1828E-02	5.8921E-03
10^{-4}	5.0063E-01	2.3021E-01	1.0696E-01	5.1049E-02	2.4870E-02	1.2266E-02
10^{-6}	7.6497E-01	3.6319E-01	1.6700E-01	7.8479E-02	3.7821E-02	1.8535E-02
10^{-8}	9.9761E-01	4.9961E-01	2.3016E-01	1.0699E-01	5.1072E-02	2.4881E-02

Table 2: Convergence rate for Example 1 using a modified graded mesh in the layer region

ε	Number of Intervals $N/\Delta\tau$
	$128/\frac{1}{10}$	$256/\frac{1}{20}$	$512/\frac{1}{40}$	$1024/\frac{1}{80}$	$2048/\frac{1}{160}$
10^{-2}	1.1158	1.0731	1.0373	1.0158	1.0053
10^{-4}	1.1057	1.1067	1.0703	1.0394	1.0207
10^{-6}	1.0447	1.1156	1.0919	1.0556	1.0302
10^{-8}	0.9509	1.1049	1.1060	1.0697	1.0391

Table 3: Maximum error on the modified graded mesh in the smooth region for Example 1

ε	Number of Intervals $N/\Delta\tau$					
	$128/\frac{1}{10}$	$256/\frac{1}{20}$	$512/\frac{1}{40}$	$1024/\frac{1}{80}$	$2048/\frac{1}{160}$	$4096/\frac{1}{320}$
10^{-2}	2.2150E-01	1.0252E-01	4.8929E-02	2.3896E-02	1.1828E-02	5.8921E-03
10^{-4}	5.0063E-01	2.3021E-01	1.0696E-01	5.1049E-02	2.4870E-02	1.2266E-02
10^{-6}	7.6497E-01	3.6319E-01	1.6700E-01	7.8479E-02	3.7821E-02	1.8535E-02
10^{-8}	9.9761E-01	4.9961E-01	2.3016E-01	1.0699E-01	5.1072E-02	2.4881E-02

Table 4: Convergence rate for Example 1 using a modified graded mesh in the smooth region

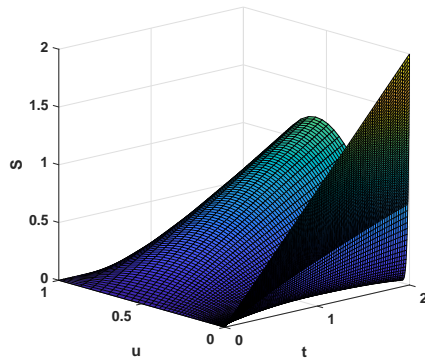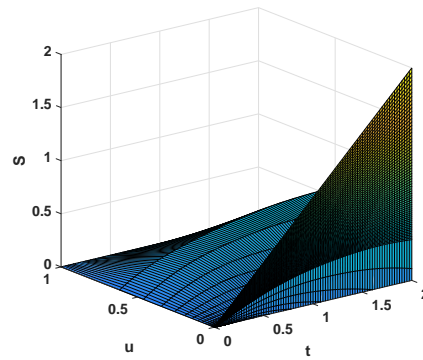| ε	Number of Intervals $N/\Delta\tau$				
	$128/\frac{1}{10}$	$256/\frac{1}{20}$	$512/\frac{1}{40}$	$1024/\frac{1}{80}$	$2048/\frac{1}{160}$
10^{-2}	1.1113	1.0672	1.0339	1.0146	1.0053
10^{-4}	1.1208	1.1058	1.0671	1.0374	1.0198
10^{-6}	1.0747	1.1209	1.0894	1.0531	1.0289
10^{-8}	0.9977	1.1182	1.1051	1.0669	1.0375

(a) $N = 128, \ \varepsilon = 10^{-2}$ (b) $N = 128, \ \varepsilon = 10^{-8}$

Figure 2: Solution profile for Example 1 for various values of N and ε

Table 5: Maximum error and rate of convergence on a modified graded mesh for Example 1

	Number of Intervals $N/\Delta\tau$					
ε	$128/\frac{1}{10}$	$256/\frac{1}{20}$	$512/\frac{1}{40}$	$1024/\frac{1}{80}$	$2048/\frac{1}{160}$	$4096/\frac{1}{320}$
10^{-2}	2.2150E-01	1.0252E-01	4.8929E-02	2.3896E-02	1.1828E-02	5.8921E-03
	1.1113	1.0672	1.0339	1.0146	1.0053	
10^{-4}	5.0063E-01	2.3021E-01	1.0696E-01	5.1049E-02	2.4870E-02	1.2266E-02
	1.1208	1.1058	1.0671	1.0374	1.0198	
10^{-6}	7.6497E-01	3.6319E-01	1.6700E-01	7.8479E-02	3.7821E-02	1.8535E-02
	1.0747	1.1209	1.0894	1.0531	1.0289	
10^{-8}	9.9761E-01	4.9961E-01	2.3016E-01	1.0699E-01	5.1072E-02	2.4881E-02
	0.9977	1.1182	1.1051	1.0669	1.0375	

(a) $N = 128$, $\varepsilon = 10^{-2}$ (b) $N = 128$, $\varepsilon = 10^{-8}$
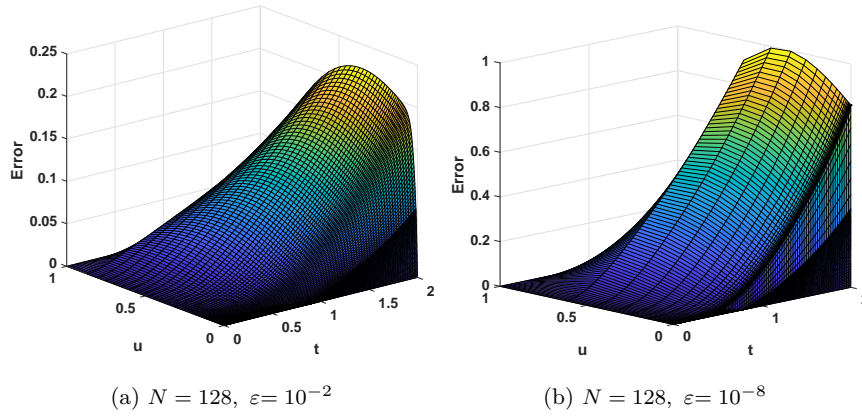
Figure 3: Error profile for Example 1 for various values of N and ε

Example 2. Consider the following problem:

$$
\begin{cases}
\hat{w}_\tau(s,\tau) - \varepsilon \hat{w}_{ss}(s,\tau) - 20\hat{w}_s(s,\tau) \\
\quad = \hat{w}(s, \tau - 1) + 10\tau^2 \exp(-\tau)s(1-s), & (s,\tau) \in (0,1) \times (0,2], \\
\hat{w}(s,\tau) = 0, & (s,\tau) \in (0,1) \times [-1,0], \\
\hat{w}(0,\tau) = 0, & \hat{w}(1,\tau) = 0, \quad \tau \in [0,2].
\end{cases}
$$

In Example 2, we do not have an exact solution. To determine the maximum pointwise error and to establish an order of convergence, we employ the double mesh principle to the computed solution. For this, we consider $2M$ and $2N$ mesh interval in the temporal and spatial directions to determine the numerical solution $\widetilde{S}(s_j, \tau_k)$ on the mesh $\bar{\aleph}^{2N} = \bar{\Lambda}_s^{2N} \times \bar{\Omega}^{2M}$, for $j = 1, 2, \ldots, N$. Additionally, the jth mesh point of Λ_s^N and the $2j$th mesh point of $\bar{\Lambda}_s^{2N}$ are identical. Furthermore, for each ε, the maximum pointwise error is defined by

$$
E_\varepsilon^{N,\Delta\tau} = \max |(S - \widetilde{S})(s_j, \tau_k)|, \quad (s_j, \tau_k) \in \aleph^N,
$$

and the order of convergence is given by

$$
\hat{p}_\varepsilon^{N,\Delta\tau} = \frac{\log(e^{N,\Delta\tau}/e^{2N,\Delta\tau/2})}{\log 2}.
$$

In Example 2, the computed maximum pointwise error is shown in Table 6, and the associated convergence order is in Table 7. The plots for the numerical solution of Example 2 for the parameters $N = 128$, $\varepsilon = 10^{-2}$ and $\varepsilon = 10^{-8}$ are shown in Figure 4a and Figure 4b. The boundary layer at $s = 0$ can be seen in these figures. Error plot of Example 2 for $N = 128$, $\varepsilon = 10^{-2}$ and $\varepsilon = 10^{-8}$ is presented in Figure 5a and Figure 5b respectively. Figure 6b is a plot of Example 2 on the log-log scale for maximum pointwise error. Table 7 and Figure 6b show that the employed scheme is first-order uniformly convergent.

Table 6: Maximum errors for Example 2 on modified graded mesh

ε	Number of Intervals $N/\Delta\tau$					
	$128/\frac{1}{10}$	$256/\frac{1}{20}$	$512/\frac{1}{40}$	$1024/\frac{1}{80}$	$2048/\frac{1}{160}$	$4096/\frac{1}{320}$
10^{-2}	1.4063E-03	6.3978E-04	2.9302E-04	1.3810E-04	6.6717E-05	3.2746E-05
10^{-4}	2.8608E-03	1.4120E-03	6.4327E-04	2.9485E-04	1.3905E-04	6.7192E-05
10^{-6}	3.8686E-03	2.1730E-03	1.0218E-03	4.6404E-04	2.1513E-04	1.0258E-04
10^{-8}	4.3736E-03	2.8588E-03	1.4119E-03	6.4336E-04	2.9491E-04	1.3906E-04

Table 7: Rate of convergence for Example 2 on a modified graded mesh

ε	Number of Intervals $N/\Delta\tau$				
	$128/\frac{1}{10}$	$256/\frac{1}{20}$	$512/\frac{1}{40}$	$1024/\frac{1}{80}$	$2048/\frac{1}{160}$
10^{-2}	1.1362	1.1266	1.0853	1.0496	1.0267
10^{-4}	1.0187	1.1343	1.1254	1.0844	1.0493
10^{-6}	0.8321	1.0885	1.1389	1.1090	1.0685
10^{-8}	0.6134	1.0178	1.1340	1.1253	1.0846

6 Conclusions

This article explored the upwind difference scheme on a modified graded mesh. Optimal error bounds were established in the maximum norm. The

(a) $N = 128$, $\varepsilon = 10^{-2}$

(b) $N = 128$, $\varepsilon = 10^{-8}$
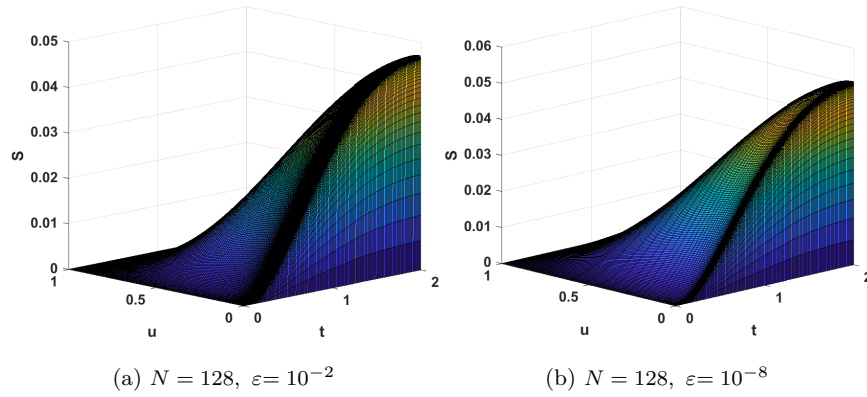
Figure 4: Solution profile for Example 2 for various values of N and ε

(a) $N = 128$, $\varepsilon = 10^{-2}$

(b) $N = 128$, $\varepsilon = 10^{-8}$
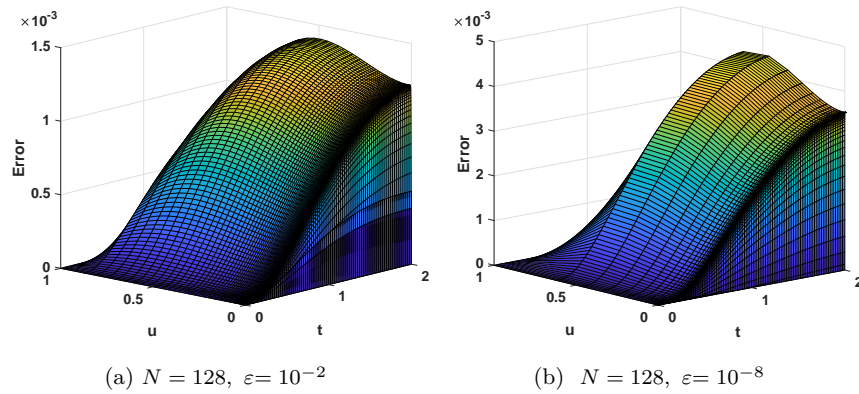
Figure 5: Error profile for Example 2 for various values of N and ε

method was proven to converge with first order up to logarithm. It can be observed from the numerical simulation that this logarithm term $\ln(1/\varepsilon)$ is not significant. Analytical estimations were carried out to gain uniform convergence results of computed solutions in the article. Two test problems were included to check the efficiency of the numerical method. Tables have been used to present the maximum pointwise error and order of convergence. Finally, numerical experiments confirmed the theoretical findings.
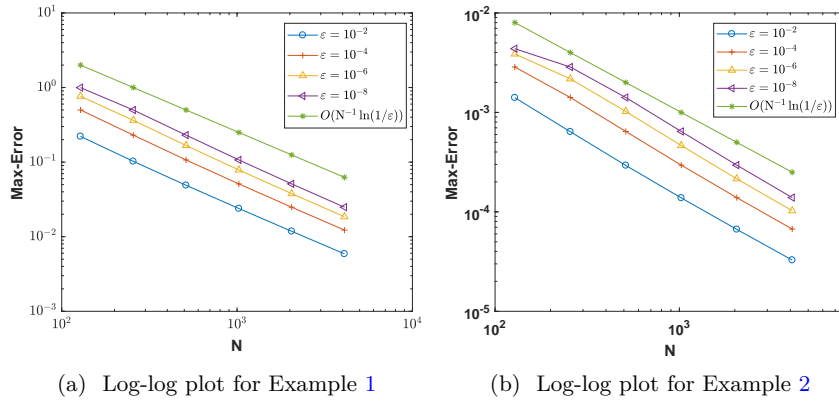
(a) Log-log plot for Example 1   (b) Log-log plot for Example 2

Figure 6: Log-log plot for Examples 1 and 2

References

[1] Ansari, A.R., Bakr, S.A. and Shishkin, G.I. *A parameter-robust finite difference method for singularly perturbed delay parabolic partial differential equations*, J. Comput. Appl. Math. 205(1) (2007), 552–566.

[2] Clavero, C., Jorge, J.C., Lisbona, F. and Shishkin, G.I.*An alternating direction scheme on a nonuniform mesh for reaction-diffusion parabolic problems*, IMA J. Numer. Anal. 20(2) (2000), 263–280.

[3] Das, A., Govindarao, L. and Mohapatra, J. *A second order weighted monotone numerical scheme for time-delayed parabolic initial-boundary-value problem involving a small parameter*, Int. J. Math. Model. Numer. Optim. 12(3) (2022), 233–251.

[4] Durán, R.G. and Lombardi, A.L. *Finite element approximation of convection diffusion problems using graded meshes*, Appl. Numer. Math. 56(10-11) (2006), 1314–1325.

[5] Elboughdiri, N., Ghernaout, D., Muhammad, T., Alshehri, A., Sadat, R., Ali, M.R. and Wakif, A. *Towards a novel EMHD dissipative stagnation point flow model for radiating copper-based ethylene glycol nanoflu-*

ids: An unsteady two-dimensional homogeneous second-grade flow case study, Case Stud. Therm. Eng. 45 (2023), 102914.

[6] Elboughdiri, N., Reddy, C.S., Alshehri, A., Eldin, S.M., Muhammad, T. and Wakif, A. *A passive control approach for simulating thermally enhanced Jeffery nanofluid flows nearby a sucked impermeable surface subjected to buoyancy and Lorentz forces*, Case Stud. Therm. Eng. (2023), 103106.

[7] Farrell, P.A., Hegarty, A.F., Miller, J.J.H., O'Riordan, E. and Shishkin, G.I. *Robust computational techniques for boundary layers*, Applied Mathematics (Boca Raton), 16. Chapman & Hall/CRC, Boca Raton, FL, 2000.

[8] Gartland, E.C. Jr., *Graded-mesh difference schemes for singularly perturbed two-point boundary value problems*, Math. Comp. 51(184) (1988), 631–657.

[9] Gowrisankar, S. and Natesan, S. *A robust numerical scheme for singularly perturbed delay parabolic initial-boundary-value problems on equidistributed grids*, Electron. Trans. Numer. Anal. 41 (2014), 376–395.

[10] Gowrisankar, S. and Natesan, S. *ε-Uniformly convergent numerical scheme for singularly perturbed delay parabolic partial differential equations*, Int. J. Comput. Math. 94(5) (2017), 902–921.

[11] Gupta, V., Kadalbajoo, M.K. and Dubey, R.K. *A parameter-uniform higher order finite difference scheme for singularly perturbed time-dependent parabolic problem with two small parameters*, Int. J. Comput. Math. 96(3) (2019), 474–499.

[12] Jha, A. and Kadalbajoo, M.K. *A robust layer adapted difference method for singularly perturbed two-parameter parabolic problems*, Int. J. Comput. Math. 92(6) (2015), 1204–1221.

[13] Kabeto, M.J. and Duressa, G.F. *Robust numerical method for singularly perturbed semilinear parabolic differential difference equations*, Math. Comput. Simulation 188 (2021), 537–547.

[14] Kuang, Y. *Delay differential equations with applications in population dynamics*, Mathematics in Science and Engineering, 191. Academic Press, Inc., Boston, MA, 1993.

[15] Kumar, D. and Kumari, P. *A parameter-uniform scheme for singularly perturbed partial differential equations with a time lag*, Numer. Methods Partial Differ. Equ. 36(4) (2020), 868–886.

[16] Kumar, K., Podila, P.C., Das, P. and Ramos, H. *A graded mesh refinement approach for boundary layer originated singularly perturbed time-delayed parabolic convection diffusion problems*, Math. Methods Appl. Sci. 44(16) (2021), 12332–12350.

[17] Kumar, S., Sumit, Vigo-Aguiar, J. *A parameter-uniform grid equidistribution method for singularly perturbed degenerate parabolic convection-diffusion problems*, J. Comput. Appl. Math. 404 (2022), Paper No. 113273, 15.

[18] Ladyženskaja, O.A., Solonnikov, V.A. and Ural ceva, N.N. *Linear and quasi-linear equations of parabolic type*, volume 23 of Translations of Mathematical Monographs. American Mathematical Society, 1968.

[19] Miller, J.J., O'riordan, E. and Shishkin, G.I., *Fitted numerical methods for singular perturbation problems: error estimates in the maximum norm for linear problems in one and two dimensions*, World Scientific, 1996.

[20] Mukherjee, K. and Natesan, S. *Richardson extrapolation technique for singularly perturbed parabolic convection-diffusion problems*, Computing 92(1) (2011), 1–32.

[21] Natesan, S. and Gowrisankar, S. *Robust numerical scheme for singularly perturbed parabolic initial-boundary-value problems on equidistributed Mesh*, CMES - Comput. Model. Eng. Sci. 88(4), (2012), 245–268.

[22] Nelson, P.W. and Perelson, A.S. *Mathematical analysis of delay differential equation models of HIV-1 infection*, Math. Biosci. 179(1) (2002), 73–94.

[23] Radojev, G. and Brdar, M. *A collocation method on a Gartland-type mesh for a singularly perturbed reaction-diffusion problem*, Math. Commun. 24(1) (2019), 19–37.

[24] Rajeev Ranjan, K. and Gowrisankar, S. *Uniformly convergent NIPG method for singularly perturbed convection diffusion problem on Shishkin type meshes*, Appl. Numer. Math. 179 (2022), 125–148.

[25] Rajeev Ranjan, K. and Gowrisankar, S. *NIPG method on Shishkin mesh for singularly perturbed convection-diffusion problem with discontinuous source term*, Int. J. Comput. Methods 20(2) (2023), Paper No. 2250048, 29 pp.

[26] Rasool, G., Wakif, A., Wang, X., Shafiq, A. and Chamkha, A.J., *Numerical passive control of alumina nanoparticles in purely aquatic medium featuring EMHD driven non-Darcian nanofluid flow over convective Riga surface*, Alex. Eng. J. 68 (2023), 747–762.

[27] Sharma, J., Ahammad, N.A., Wakif, A., Shah, N.A., Chung, J.D. and Weera, W. *Solutal effects on thermal sensitivity of casson nanofluids with comparative investigations on Newtonian (water) and non-Newtonian (blood) base liquids*, Alex. Eng. J. 71 (2023), 387–400.

[28] Shishkin, G.I. *Robust novel high-order accurate numerical methods for singularly perturbed convection-diffusion problems*, Math. Model. Anal. 10(4) (2005), 393–412.

[29] Villasana, M. and Radunskaya, A. *A delay differential equation model for tumor growth*, J. Math. Biol. 47(3) (2003), 270–294.

[30] Wakif, A. *Numerical inspection of two-dimensional MHD mixed bioconvective flows of radiating Maxwell nanofluids nearby a convectively heated vertical surface*, Waves Random Complex Media, (2023), 1–22.

[31] Wakif, A., Abderrahmane, A., Guedri, K., Bouallegue, B., Kaewthongrach, R., Kaewmesri, P. and Jirawattanapanit, A., *Importance of exponentially falling variability in heat generation on chemically reactive*

von kármán nanofluid flows subjected to a radial magnetic field and controlled locally by zero mass flux and convective heating conditions: a differential quadrature analysis, Front. Phys. 10 (2022), 988275.

[32] Wu, J. *Theory and applications of partial functional-differential equations*, Applied Mathematical Sciences, 119. Springer-Verlag, New York, 1996.

[33] Zhang, K., Shah, N.A., Alshehri, M., Alkarni, S., Wakif, A. and Eldin, S.M. *Water thermal enhancement in a porous medium via a suspension of hybrid nanoparticles: MHD mixed convective Falkner's-Skan flow case study*, Case Stud. Therm. Eng. 47 (2023), 103062.